NANOSYSTEMS:
PHYSICS, CHEMISTRY, MATHEMATICS

Original article

Avdeeva Yu.A., et al. *Nanosystems: Phys. Chem. Math.*, 2023, **14** (1), 132–141.
http://nanojournal.ifmo.ru
DOI 10.17586/2220-8054-2023-14-1-132-141

Plasma-chemical synthesis of nanocrystalline "core-shell" structures TiN–Mo–Co

Yuliya A. Avdeeva[1,a], Irina V. Luzhkova[1,b], Aidar M. Murzakaev[2,c], Alexey N. Ermakov[1,d]

[1]Institute of Solid State Chemistry, Ural Branch, Russian Academy of Sciences, Ekaterinburg, Russia
[2]Institute of Electrophysics, Ural Branch, Russian Academy of Sciences, Ekaterinburg, Russia

[a]y-avdeeva@list.ru, [b]key703@yandex.ru, [c]aidar@iep.uran.ru, [d]ermakovihim@yandex.ru

Corresponding author: Yuliya A. Avdeeva, y-avdeeva@list.ru

PACS 61.46.+w, 61.46.-w, 61.66.Fn

ABSTRACT In this work, the possibilities of formation of nanocrystalline powders based on titanium nitride with participation of Mo and Co under conditions of plasma-chemical synthesis have been studied. Synthesis was performed according to the plasma recondensation scheme using low-temperature nitrogen plasma. All the obtained highly dispersed powders were certified by X-ray diffraction and scanning electron microscopy. The characteristics of the disperse composition of the recondensed TiN–Mo–Co products were determined by the calculation based on the pycnometric density and specific surface area data.

The possibility of formation of a "core-shell" structure was confirmed using chemical methods by etching ultra- and nanodispersed powders in solutions of dilute HCl to remove the cobalt shell and concentrated hydrogen peroxide H_2O_2 to neutralize metallic Mo.

Based on the information about "quasi-equilibrium state" of the products of plasma-chemical synthesis in a low-temperature gas plasma, a chemical model for the formation of nanocrystalline particles is proposed.

KEYWORDS core-shell structure, titanium nitride, plasma-chemical synthesis, temperature barrier, phase formation

ACKNOWLEDGEMENTS The authors are grateful to Dr. E. K. Dobrinsky, Ph. D., leading researcher of SSC RF JSC "GNIIChTEOS" for help in carrying out the plasma-chemical synthesis. The work was carried out in accordance with the state assignment for the Institute of Solid State Chemistry of the Ural Branch of the Russian Academy of Sciences (theme No 0397-2019-0003 "New functional materials for promising technologies: synthesis, properties, spectroscopy and computer simulation").

FOR CITATION Avdeeva Yu.A., Luzhkova I.V., Murzakaev A.M., Ermakov A.N. Plasma-chemical synthesis of nanocrystalline "core-shell" structures TiN–Mo–Co. *Nanosystems: Phys. Chem. Math.*, 2023, **14** (1), 132–141.

1. Introduction

Compounds based on titanium nitride are widely used as refractory bases for tool and structural materials, as well as decorative coatings that are resistant to aggressive chemical environments. Of particular interest to researchers is the nanocrystalline state of titanium nitride, formed under the conditions of various methods of extreme exposure, which have high productivity. Such methods include mechanical dispersion performed in high-speed attritors [1], detonation synthesis [2], plasma-chemical synthesis in low-temperature gas (including nitrogen) plasma [3], electrical explosion of a conductor in a controlled gas atmosphere [4], etc.

In the present work, an attempt was made to form a core-shell structure of TiN–Mo–Co under the conditions of plasma-chemical synthesis according to the plasma recondensation scheme. Recondensation is based on the effect of crystallization of evaporated mechanical mixtures in an intensely swirling nitrogen flow in a quenching chamber, followed by separation of the synthesis products into fractions. The products are separated in a vortex-type cyclone and a fabric bag filter.

As previous studies show, the use of plasma-chemical synthesis for the recondensation of microcrystalline materials, such as titanium nickelide [5] or mechanical mixtures based on TiC [6], VC, VN [7] with metallic nickel, allows the formation of "core-shell" structures. A refractory compound based on elements of IV-VIA subgroups of the Periodic Table acts as the core, and the peripheral shell is presented in the form of Ni of cubic modification. It should be noted that under such extreme conditions, during recondensation in a tangential flow of nitrogen at a rate of 10^5 °C/s, processes occur that cannot be carried out at lower crystallization rates. One of these processes is deposition of metallic nickel on ultra- and nanodispersed particles of titanium and vanadium nitrides. There is information in the literature [8] that the contact angles of wetting of complete nitride compounds of IV-VIA subgroup elements with nickel melts exceed 90°, meaning their complete non-wettability. At the same time, according to [8], highly defective titanium and vanadium nitrides ($\sim TiN_{0.7}$) are characterized by wetting. Thus, under conditions of plasma recondensation, a layer of metallic

nickel can be formed either due to strong nonstoichiometric nature of the core of the refractory base, or in the presence of an interface layer, the phase composition of which should include elements contained both in the grain and on its periphery. Indeed, the X-ray diffraction experiments revealed the presence of highly deformed, according to [9], titanium-nickel nitride $Ti_{0.7}Ni_{0.3}N$ [10] and presumably its analogue $V_{0.7}Ni_{0.3}N$, information about which is not available in X-ray databases. The presence of detected complex intermetallic compounds is in good agreement with the theory of B. Chalmers [11], corrected for the nanocrystalline state in [12].

2. Methods

Plasma-chemical synthesis (Saratov, branch of SSC RF JSC "GNIIChTEOS") in low-temperature (4000 – 6000 °C) nitrogen plasma with subsequent recondensation in a tangential flow of nitrogen gas is proposed as the main method for the synthesis of ultra- and nanodispersed "core-shell" TiN–Mo–Co structures. The cooling rate in this case can reach the values of 10^5 °C/s. The description of the synthesis procedure itself and its technological parameters are given in [3] and Table 1. It is also indicated that at the final stage encapsulation of ultradispersed and nanocrystalline synthesis products in organic vapors is envisaged, which makes it possible to reduce the chemical activity and pyrophoricity of the resulting powders, especially in a highly dispersed state.

TABLE 1. Technical parameters of plasma-chemical installation

Precursor mixture consumption, g/h	200
Plasma torch power, kW	25
Current strength, A	100 – 110
Voltage, V	200 – 220
Plasma flow rate, m/s	60 – 100
Total nitrogen consumption in the plasma reactor, nm^3/h	25 – 30
Out of the total nitrogen consumption for plasma formation, nm^3/h	6
Out of the total nitrogen consumption for stabilization and hardening, nm^3/h	19 – 16

All the obtained ultrafine and nanocrystalline powders TiC–Mo–Co were studied by X-ray diffraction (X-ray diffractometer Shimadzu XRD 7000, CuKα-cathode) and scanning electron microscopy (Scanning electron microscope JEOL JSM 9390, W-cathode) taking into account energy dispersive analysis data (analyzer JEM-2300). The phase composition and crystallographic characteristics were refined using the WinXPOW and PowderCell 2.3 software products oriented to the use of the ICDD and ISCD databases.

Additionally, to obtain the information about the physical characteristics (density, specific surface area, porosity and calculated average particle size), studies were carried out on a helium pycnometer (AccuPyc II 1340 V1.09) and a specific surface analyzer using the BET method (Gemini VII 2390 V1.03 (V1.03 t)). The calculation of the average particle size was carried out according to formula (1):

$$d_{\mathrm{av}} = \frac{6}{S_{\mathrm{sp}}\rho}, \tag{1}$$

where d_{av} is the average particle diameter, S_{sp} is the specific surface area determined by the BET method, ρ is the pycnometric density of the powder fraction determined on a helium pycnometer.

According to the results of high-resolution transmission electron microscopy on electron microscopy images, direct measurements of nanocrystalline particles were carried out using the software product MEASURER (own development of the Institute of Solid State Chemistry, UB RAS). Based on the results of measurements of the widths and heights of individual particles, a sample was formed. It was used to determine the particle diameters in accordance with the Pythagorean formula. Further, using the ORIGIN software, the average particle size was determined and a histogram of the size distribution was constructed, described by the lognormal law. The measurement accuracy and the error value were up to 0.1 nm, taking into account the significant sample size and the nanocrystalline state of the plasma-chemical powder.

3. Results and discussion

The results of the X-ray studies of recondensed nanocrystalline powders are presented in Table 2.

According to the results of X-ray diffraction, it can be seen (Table 2) that all ultrafine and nanocrystalline powders in the TiN–Mo–Co system are multiphase. The phase composition is characterized by the presence of refractory compounds based on titanium and molybdenum; individual metallic Mo and Co are also presented. Thus, all singly and doubly recondensed fractions from the cyclone and the filter contain refractory interstitial phases based on titanium nitride with

TABLE 2. Physicochemical properties of powder fractions recondensed from TiN–Mo–Co mechanical mixture taking into account etching in boiling HCl

No	Fraction	Phase composition, wt. %, a, b, c, (± 0.0001 Å)	ρ, g/cm^3	S_{sp}, m^2/g	d_{av}, μm
1	1TiN–Mo–Co (cyclone)	Co (Fm-3m), (26.93 %), $a = 3.5440$; $Ti_{1-n}Mo_nC_xN_y$ (Fm-3m), (43.89 %), $a = 4.2419$; Mo (Im-3m), (4.79 %), $a = 3.1463$; $Mo_{0.42}C_{0.58}$ (Pnnm), (14.06 %), $a = 5.1367$, $b = 4.7997$, $c = 2.9722$; TiO_2 (P42/mnm), (10.33 %), $a = 4.5845$, $c = 2.9615$	5.6365	3.0301	0.351
2	1TiN–Mo–Co (filter)	Co (Fm-3m), (49.87 %), $a = 3.5469$; $Ti_{1-n}Mo_nC_xN_y$ (Fm-3m), (8.96 %), $a = 4.2444$; Mo (Im-3m), (1.37 %), $a = 3.1479$; $Mo_{0.42}C_{0.58}$ (Pnnm), (8.69 %), $a = 5.1380$, $b = 4.8040$, $c = 2.9713$; TiO_2 (P42/mnm), (31.12 %), $a = 4.5897$, $c = 2.9586$	5.7776	9.3973	0.110
3	2TiN–Mo–Co (cyclone)	Co (Fm-3m), (33.08 %), $a = 3.5473$; $Ti_{1-n}Mo_nC_xN_y$ (Fm-3m), (44.01 %), $a = 4.2463$; Mo (Im-3m), (4.63 %), $a = 3.1495$; $Mo_{0.42}C_{0.58}$ (Pnnm), (8.13 %), $a = 5.1028$, $b = 4.7763$, $c = 2.9910$; TiO_2 (P42/mnm), (10.16 %), $a = 4.5937$, $c = 2.9570$	5.8973	3.9784	0.255
4	2TiN–Mo–Co (filter)	Co (Fm-3m), (41,54 %), $a = 3.5474$; $Ti_{1-n}Mo_nC_xN_y$ (Fm-3m), (14.71 %), $a = 4.2463$; Mo (Im-3m), (2.97 %), $a = 3.1492$; $Mo_{0.42}C_{0.58}$ (Pnnm), (17.34 %), $a = 5.1466$, $b = 4.7906$, $c = 2.9770$; TiO_2 (P42/mnm), (10.33 %), $a = 4.5883$, $c = 2.9668$	5.7617	10.0729	0.103
Etching in boiling HCl (1 hour)					
5	1TiN–Mo–Co (cyclone)	Mo (Im-3m), (5.31 %), $a = 3.1470$; TiC_xO_z (Fm-3m), (72.47 %), $a = 4.2423$ TiO_2 (P42/mnm), (22.22 %), $a = 4.5901$, $c = 2.9598$	4.8937	2.5772	0.475
6	1TiN–Mo–Co (filter)	$Mo_{0.42}C_{0.58}$ (Pnnm), (2.43 %), $a = 5.1566$, $b = 4.8321$, $c = 2.9690$; Mo (Im-3m), (2.38 %), $a = 3.1444$; TiN_xO_z (Fm-3m), (23.95 %), $a = 4.2361$; TiO_2 (P42/mnm), (71.23 %), $a = 4.5944$, $c = 2.9600$	4.5530	21.6385	0.060
7	2TiN–Mo–Co (cyclone)	Mo (Im-3m), (9.41 %), $a = 3.1492$; TiC_xO_z (Fm-3m), (74.53 %), $a = 4.2456$; TiO_2 (P42/mnm), (16.06 %), $a = 4.5901$, $c = 2.9565$	5.2179	4.3632	0.263
8	2TiN–Mo–Co (filter)	$Mo_{0.42}C_{0.58}$ (Pnnm), (2.12 %), $a = 5.1562$, $b = 4.8321$, $c = 2.9654$; Mo (Im-3m), (5.63 %), $a = 3.1443$; TiC_xN_y (Fm-3m), (28.31 %), $a = 4.2463$; TiO_2 (P42/mnm), (63.94 %), $a = 4.5937$, $c = 2.9565$	4.1689	17.8331	0.080

carbon TiC_xN_y ($x + y < 1$) (sp. gr. Fm-3m), in agreement with the data of [13]. The percentage of TiC_xN_y ($x + y < 1$), according to semi-quantitative analysis, sharply decreases from the cyclone to the filter (Table 2, Nos. 1–4). All the recondensed powder materials contain metallic Mo of the cubic modification (sp. gr. Im-3m), the content of which decreases from the cyclone to the filter for both recondensation options. Besides, the core-shell structures contain highly defective molybdenum carbide $Mo_{0.42}C_{0.58}$ (sp. gr. Pnnm) described by Novotny et al. in [14]. Its quantitative indicators increase from the corresponding fractions from the cyclone to the filter, which is also reflected in Table 2, Nos. 1–4. The formation of $Mo_{0.42}C_{0.58}$ carbide is due to the fact that the proposed study is part of an extensive scientific work aimed at obtaining highly dispersed "core-shell" structures, where titanium carbides and nitrides are considered as cores, including those alloyed with molybdenum in the metal sublattice. At the same time, it should be noted that the plasma-chemical installation was not cleaned when the charge materials with the carbide component were changed to those with the nitride component. Under these conditions, the formation of highly defective molybdenum carbide $Mo_{0.42}C_{0.58}$ (sp. gr. Pnnm) and titanium carbonitrides TiC_xN_y (sp. gr. Fm-3m) enriched in nitrogen in the nonmetallic sublattice is quite natural. The metal phase component of all TiN–Mo–Co nanocrystalline "core-shell" structures is also supplemented by the presence of cubic cobalt (sp. gr. Fm-3m), the quantitative content of which also increases from the cyclone to the filter (Table 2, Nos. 1–4). Additionally, it should be noted that the composition of nanocrystalline powders includes titanium-cobalt nitride $Ti_{0.7}Co_{0.3}N$ of hexagonal modification (sp. gr. P-6m2), which was first described in [15, 16]. Under the conditions of plasma-chemical synthesis, which refer to extreme methods of influencing crystalline substances, during recrystallization in a tangential flow of gaseous nitrogen at a speed of 10^5 °C/s, this phase is in a highly deformed state, in accordance with [9]. This state is characterized by a forced preferential orientation along the (101) plane, which is one of the most intense orientations in the P-6m2 space group. The forced orientation of the $Ti_{0.7}Co_{0.3}N$ phase does not allow one to refine the unit cell parameters and determine its quantity.

TiO_2 is included in the composition to reduce the pyrophoricity of ultra- and nanodispersed powders of plasma-chemical synthesis. Its amount increases significantly after single recondensation, and changes little if at all after double processing (Table 2, Nos. 1-4).

For a more accurate determination of the phase composition of the "core-shell" structures, chemical etching was carried out in a boiling solution of dilute (1:1) HCl for 1 hour. According to the results of X-ray phase analysis (Table 2, Nos. 5–8), metallic cobalt and highly defective $Mo_{0.42}C_{0.58}$ in the fractions from the cyclone (Table 2, Nos. 5–7) were completely dissolved during boiling. It was also noted that during boiling in acid, the unit cell parameters of TiC_xN_y ($x + y < 1$) slightly changed, but in accordance with [13], the chemical composition did not undergo any significant changes. Thus, the refractory ceramic base of all "core-shell" structures is represented by titanium nitride with nitrogen positions partially replaced by carbon in the non-metallic sublattice, while the sum $x + y$ is less than 1. Since the ratio of phase components changed, the amount of metallic Mo (sp. gr. Im-3m) and TiO_2 (sp. gr. P42/mnm) of the rutile modification increased in the etched samples. On the other hand, as is known from [17], metallic molybdenum does not dissolve in dilute HCl, and an increase in the amount of TiO_2 can be associated with partial acidification of nanosized titanium carbonitride TiC_xN_y ($x + y < 1$) during boiling.

Based on the data of X-ray phase analysis (Table 2) of TiN–Mo–Co powders, by comparing the conditions for their production using plasma-chemical technology with some physicochemical laws of the formation of refractory compounds and the conditions for their wetting with metallic media, it is possible to carry out physicochemical modeling of the processes of formation of "core-shell" structures. The chemical model is based on refractory titanium compounds coated with molybdenum and cobalt metal phases and takes into account the formation of highly defective carbide $Mo_{0.42}C_{0.58}$ and complexly substituted metastable nitride $Ti_{0.7}Co_{0.3}N$ [5] (Fig. 1).

Since the working temperature of the evaporation processes in the plasma-chemical reactor is 4000 – 6000 °C, and the crystallization rate in a tangential flow of nitrogen gas in the hardening chamber is 10^5 °C/s, the formation of "core-shell" structures can be modeled only as a function of temperature variation throughout the quenching chamber. Thus, the quenching chamber can be separated by temperature barriers corresponding to crystallization temperatures of the phase components, determined and refined according to the data of X-ray phase analysis. In accordance with [12, 18, 19], a low-temperature gas plasma can be considered as "quasi-equilibrium". The formation conditions can also be considered "quasi-equilibrium" because the Arrhenius law is observed. In this case, the sequence of formation of nanocrystalline layers of TiN–Mo–Co "core-shell" structures can be determined based on the evaporation and crystallization temperatures of the phase components determined by X-ray diffraction, as well as $\Delta G(T)$ dependencies for refractory compounds that are part of highly dispersed powders. For all phase components, with the exception of highly defective molybdenum carbide $Mo_{0.42}C_{0.58}$ and metastable complex nitride $Ti_{0.7}Co_{0.3}N$, the evaporation and crystallization temperatures are presented in Table 3, and $\Delta G(T)$ dependences in Fig. 2.

The temperature of 4000 °C can be considered as the first temperature barrier of the "core-shell" structure formation model (Fig. 1), since this temperature is the minimum when plasma-chemical synthesis is carried out in low-temperature nitrogen plasma (4000 – 6000 °C) with subsequent recondensation. On passing this temperature, in accordance with [5], Mo and Ti are presented simultaneously in the gaseous and liquid state, while C and Co are in the gaseous form, and TiN is in the liquid form. As the second temperature barrier, corresponding to the melting temperature of titanium nitride TiN (2930 °C [20]), is approached, it can be assumed that titanium carbonitride, in which the nitrogen content significantly

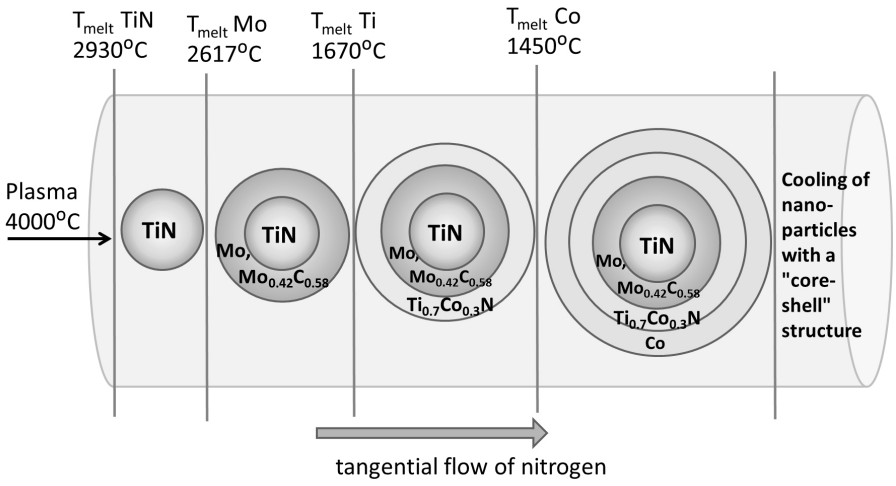

FIG. 1. Chemical mechanism of formation of TiN–Mo–Co "core-shell" structures

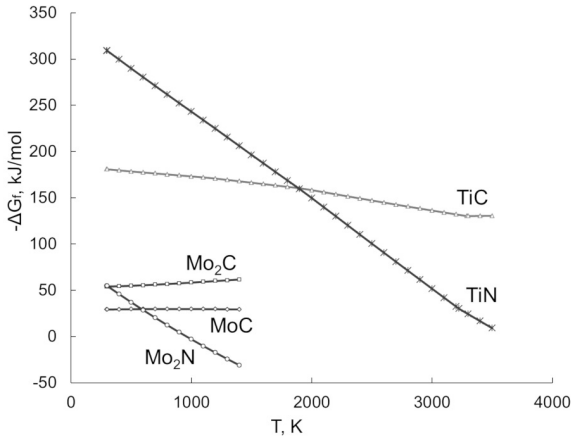

FIG. 2. $-\Delta G_f(T)$ dependences for Mo_2N, MoC, Mo_2C, TiN and TiC compounds

TABLE 3. Boiling and melting points of phase components in the TiN–Mo–Co system

Component	T_{melt}, °C	T_{boil}, °C
TiN	2930	—
TiC	3300	4300
Mo	2617	4885
Ti	1670	3287
MoC	2700	—
MoN	1750	
Co	1485	2870

exceeds the carbon content (Table 2, Nos. 1–4), crystallizes. At the same time, etching in HCl promotes a change in the lattice parameters of titanium carbide-nitride compounds for the corresponding fractions. So, for example, for singly recondensed fractions from the cyclone, the unit cell parameter increases from 4.2419 to 4.2423 Å (Table 2, Nos. 1,5), and that from the filter decreases from 4.2444 to 4.2361 Å (Table 2, Nos. 2,6). Under conditions of double recondensation, analogous parameters for the fractions from the cyclone, taking into account etching, decrease slightly from 4.2463 to 4.2456 Å (Table 2, Nos. 3,7), while for the fractions from the filter they do not change and are equal to 4.2463 Å (Table 2, Nos. 4,8).

Based on the patterns of formation of solid solutions used in the plasma-chemical synthesis of elements, it can be said that after a single recondensation (Table 2, Nos. 1, 2), a fraction is concentrated in the cyclone, in which the refractory phase based on titanium nitride is saturated with carbon. In the fraction from the filter, molybdenum is presented in the metal sublattice of carbonitride with the formation of a $Ti_{1-n}Mo_nC_xN_y$ solid solution. Under the conditions of double recondensation (Table 2, Nos. 3,4), as mentioned above, no changes in the unit cell parameters of the refractory base of the "core-shell" structures are observed and their phase composition, in accordance with [13], can be described by the formula $TiC_{0.12}N_{0.77}$. Boiling in a hydrochloric acid solution, in addition to the dissolution of cobalt, which is the surface layer in all core-shell structures, can also contribute to the oxidation of the refractory base of all ultra- and nanodispersed powder fractions under study. In accordance with [13], after a single recondensation, titanium oxycarbide $TiC_{0.21}O_{0.8}$ was recorded in the fraction from the cyclone (Table 2, No. 5), and titanium oxynitride $TiN_{0.52}O_{0.34}$ – in the fraction from the filter (Table 2, No. 6). Etching of doubly recondensed powders, according to the results of X-ray phase analysis, contributed to the formation of titanium oxycarbide $TiC_{0.21}O_{0.8}$ [13] (Table 2, No. 7) in the cyclone. In the fraction from the filter, as expected, it was not possible to fix phases of the composition Ti–C–O and Ti–N–O (Table 2, No. 8) due to their complete oxidation to TiO_2 of the rutile modification, the content of which reaches 63.94 wt. %, and the refractory base is represented by titanium carbonitride having the composition $TiC_{0.12}N_{0.77}$ [13].

The third temperature barrier can start from the crystallization temperature of metallic molybdenum, which is 2617 °C [8]; at this temperature, Mo crystallizes in a cubic bcc cell. Highly defective molybdenum carbide $Mo_{0.42}C_{0.58}$ of the orthorhombic modification crystallizes as an additional phase. Its formation is due to the presence of free carbon in the recondensable system, which is presented in the described temperature range. In accordance with Fig. 2, combining the data from [21], MoN is formed at $\Delta G(T)$ values close to 0, which is virtually impossible in the presented core-shell structures due to the extremely high cooling rate in a gaseous medium and the crystallization temperature of MoN (1750 °C [8]) compared with Mo.

The fourth temperature barrier corresponds to the formation temperature (1670 °C [8]) of a complex nitride containing Ti, Co, and N in its composition in accordance with [15]. In particular, at the onset of this temperature regime, in the process of chemical interaction, from the residual amounts of titanium that did not have time to react with nitrogen earlier, a metastable phase in the form of a complexly substituted nitride $Ti_{0.7}Co_{0.3}N$ is formed in a complex with molten Co [15]. This phase, as described earlier in [9], is in a highly deformed state due to the use of an extreme synthesis technique, which includes plasma-chemical synthesis in low-temperature nitrogen plasma. The forced orientation of $Ti_{0.7}Co_{0.3}N$ along the (101) direction ensures positive wettability of the nanocrystalline "core-shell" structures by metallic cobalt when passing the final fifth temperature barrier, the temperature of which specifies the crystallization of metallic cobalt (1450 °C [8]).

The described chemical model (Fig. 1) for the formation of nanocrystalline particles involving titanium nitride, metallic molybdenum, and cobalt is well confirmed by high-resolution transmission electron microscopy data. In particular, Fig. 3(a,b) show electron microscopic images illustrating the dispersity of the studied nanocrystalline fraction, and Fig. 2(c) demonstrates a size distribution histogram of the measured particles, on the basis of which it was found that, according to the results of measurements of 8598 particles, the average size was 34.64 ± 0.18 nm, which is much less than the calculated data given in Table 2, No. 4.

The "core-shell" structure is visualized in Fig. 4, where it is clearly seen that the coating of the core is continuous and has a uniform thickness. Fig. 3(b) shows a FFT pattern with a banded contrast with an interplanar spacing of 0.25 nm corresponding to the (111) plane of cubic TiN (sp. gr. Fm-3m). In addition, the plane of rutile (110) TiO_2 (sp. gr. P42/mnm) was determined in section 2 of Fig. 4(a, c) with an interplanar spacing of 0.33 nm.

Further, Fig. 5(a) shows a nanocrystalline particle with a core-shell structure. The core of the presented particle is characterized by moire contrast, the presence of which indicates the diffracting planes of the crystal lattice, which overlap and can have different interplanar spacing and orientation. Fig. 5(c) shows the FFT-transformation of region 1 of the core (Fig. 5(b)), where the interplanar distances of 0.25 and 0.21 nm were determined, which correspond to the (011) and (120) planes of highly defective carbide $Mo_{0.42}C_{0.58}$ of the orthorhombic modification (sp. gr. Pnnm). Additionally, $Ti_{0.7}Co_{0.3}N$ nitride, to which the (001) plane with an interplanar spacing of 0.29 nm belongs, was determined in section 1 (Fig. 5(b,c)). Using the Fourier transform of the shell (Fig. 5(d)), which corresponds to the banded contrast in region 2 (Fig. 5(b)), the interplanar spacing was determined to be 0.24 nm, corresponding to the (212) plane of metallic Co (sp. gr. P63mc).

Possible deviations of the values of interplanar distances of highly defective molybdenum carbide from the data of the ICDD and ICSD file cabinets are due to the fact that the powders studied in the work were obtained under extreme

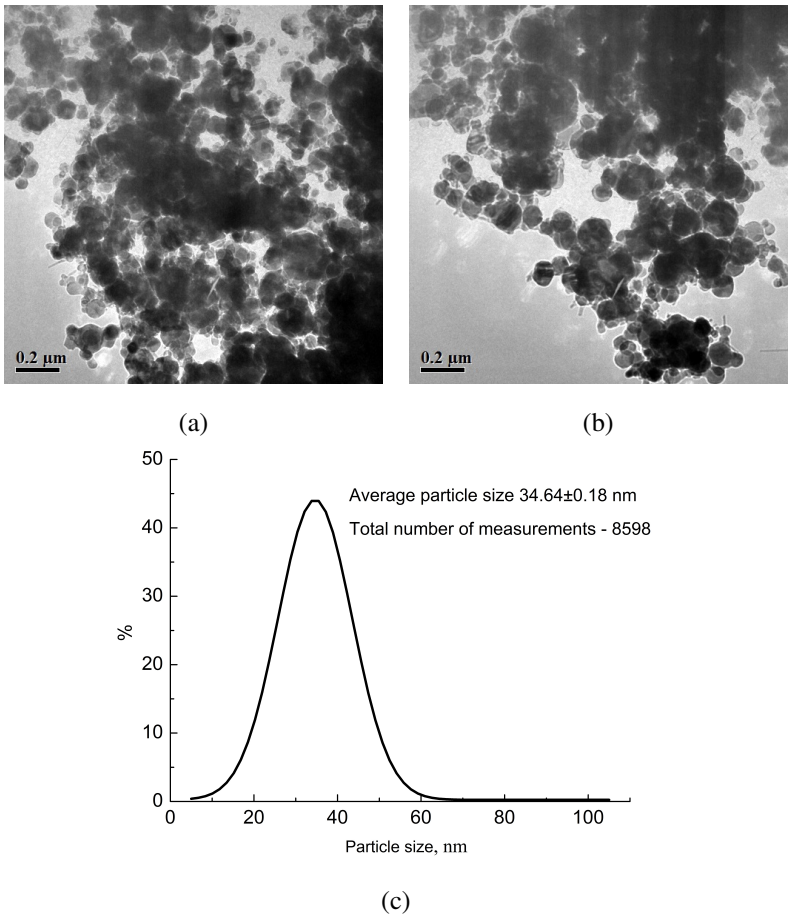

FIG. 3. Electron microscopic images of sections of TiN–Mo–Co fractions (a, b) and a histogram of particle size distribution (c)

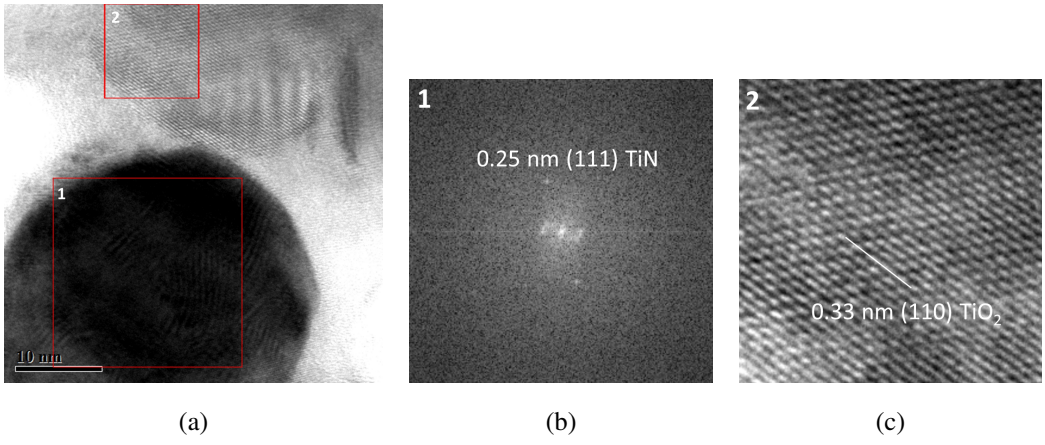

FIG. 4. Electron microscopic image of a section of the TiN–Mo–Co fraction (a), the Fourier transform of section 1 (b), enlarged image of section 2 (c)

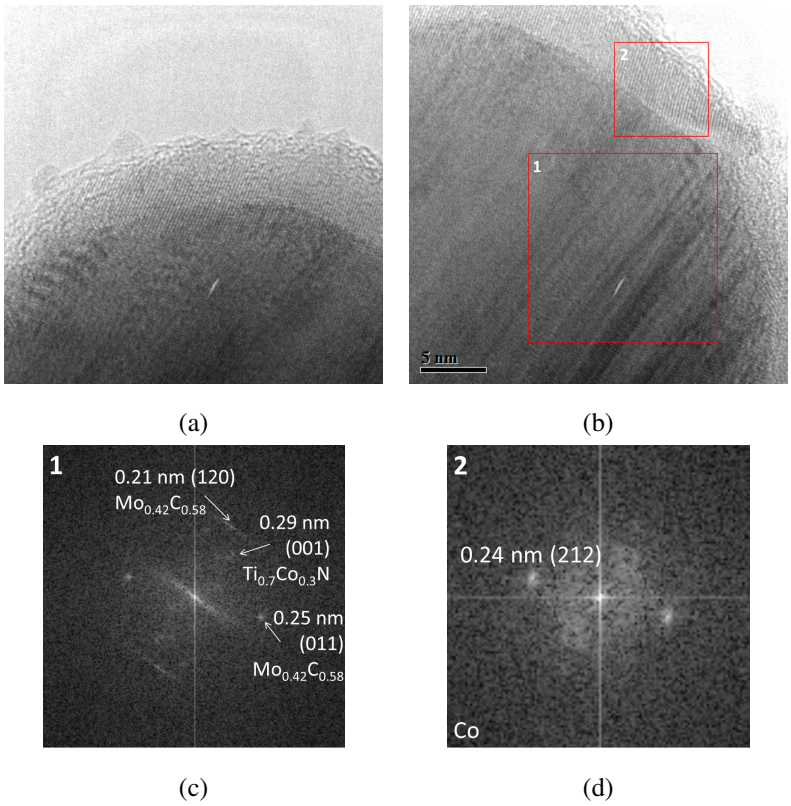

FIG. 5. HR TEM image of a TiN–Mo–Co particle (a, b), the Fourier transforms of sections 1 (c) and 2 (d)

conditions of plasma-chemical synthesis. This, in turn, creates microdeformations in the crystal lattice of $Mo_{0.42}C_{0.58}$ and contributes to its distortion.

From the results of plasma-chemical synthesis and X-ray diffraction of the obtained products it can be said that the formation of rutile TiO_2 is due to forced acidification in storage devices of separators aimed to reduce the pyrophoricity of highly dispersed TiN–Mo–Co fractions. At the same time, the HR TEM results show that some of the nanocrystalline particles with the "core-shell" structure are almost completely oxidized to TiO_2. However, in some cases, as shown in Fig. 6, carbon planes are registered (Fig. 6(b)). The Fast Fourier transform of section 1 presented in Fig. 6(a, b) illustrates the presence of TiO_2 (sp. gr. Pbca) at interplanar distances of 0.34 and 0.41 nm, which corresponds to the (111) and (020) planes. Carbon of the hexagonal modification (space group P63/mmc) was visualized on the Fourier transform (Fig. 6(c)) with an interplanar spacing of 0.33 nm, which corresponds to the (002) plane.

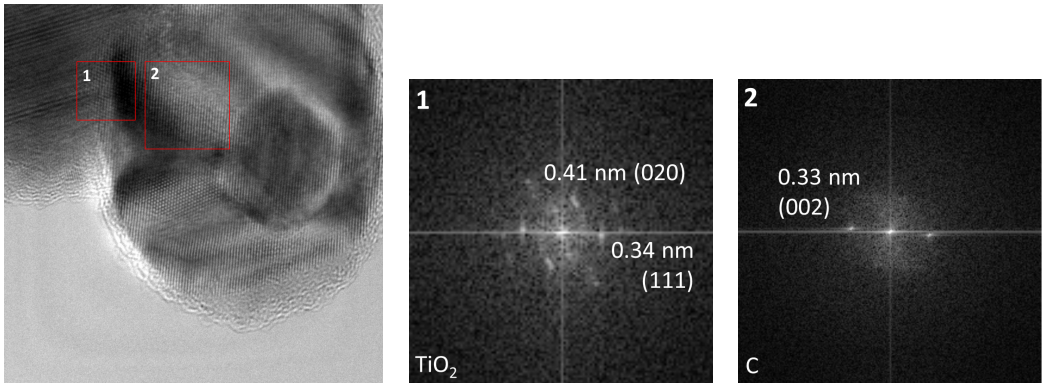

FIG. 6. HR TEM image of a TiN–Mo–Co particle (a), the Fourier transforms of sections 1 (b) and 2 (c)

In accordance with the theory of heterogeneous nucleation by Chalmers B. [11], the metallic component of Co is located on the surface of "core-shell" particles. Based on the analysis of the above electron microscopic images of TiC–Mo–Co nanoparticles, we can say that the cobalt shell (Figs. 5(d), 7(c)) is a pseudo-amorphous coating on the particle surface.

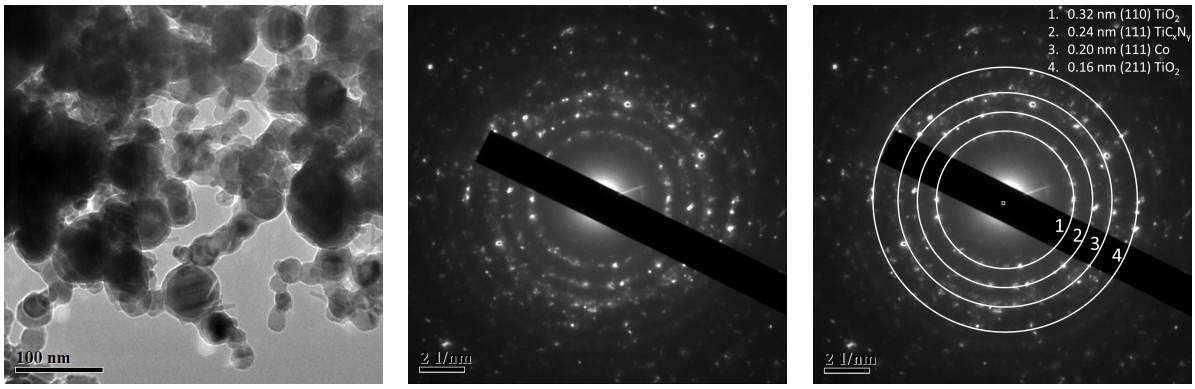

(a) (b) (c)

FIG. 7. Electron diffraction pattern (b, c) of the area (a) of TiN–Mo–Co fractio

To unambiguously confirm the presence of all X-ray diffraction-defined phase components, electron diffraction studies were carried out on a polycrystalline sample (Fig. 7). During the identification of electron diffraction projections, the presence of the following phase components was confirmed: the rutile modification of TiO_2 (sp. gr. P42/mnm) was determined from interplanar distances of 0.32 and 0.16 nm, which corresponds to the (110) and (211) planes; the cubic titanium carbonitride TiC_xN_y (sp. gr. Fm-3m) enriched with nitrogen in the non-metallic sublattice was fixed at an interplanar distance of 0.24 nm, which corresponds to the (111) plane. Metallic Co of the cubic modification (sp. gr. Fm-3m) was determined by the interplanar spacing of 0.20 nm, which corresponds to the (111) plane.

4. Conclusions

Ultrafine and nanocrystalline powders TiN–Mo–Co have been obtained by plasma-chemical synthesis in low-temperature nitrogen plasma from a mechanical mixture based on titanium nitride TiN with the participation of metallic molybdenum and cobalt.

The resulting powders were studied by X-ray diffraction and high-resolution transmission electron microscopy. It was established that under the conditions of plasma-chemical synthesis, ultrafine and nanocrystalline powder fractions are formed, which include titanium nitrides and carbonitrides, cobalt, molybdenum and its highly defective carbide $Mo_{0.42}C_{0.58}$ of the orthorhombic modification, as well as titanium oxide TiO_2 of the rutile modification.

In some cases, HR TEM images show the presence of free carbon of hexagonal modification (sp. gr. P63/mmc), and nanocrystalline grains are core-shell structures. Refractory titanium compounds act as the core, and metallic molybdenum and cobalt as the shell.

References

[1] Vereshchagin M.N., Goranskij G.G., Kiriluk S.I., Agunovich I.V. Investigation of processes of structure and phase formation of blend powders on the basis of waste of hard tungsten-containing alloys at their mechano-synthesis and high-speed mechanical dispersing for production of powder compositions. *Litiyo i Metallurgiya (Foundry Production and Metallurgy)*, 2012, **1** (84), P. 110–114.

[2] Langenderfer M.J., Fahrenholtz W.G., Chertopalov S., Zhou Y., Mochalin V.N., Johnson C.E. Detonation synthesis of silicon carbide nanoparticles. *Ceram. Int.*, 2020, **46** (5), P. 6951–6954.

[3] Storozhenko P.A., Guseinov Sh.L., Malashin S.I. Nanodispersed powders: synthesis methods and practical applications. *Nanotech. in Russia*, 2009, **4**, P. 262–274.

[4] Lerner M.I., Glazkova E.A., Lozhkomoev A.S., Svarovskay N.V., Bakina O.V., Pervikov A.V., Psakhie S.G. Synthesis of Al nanoparticles and Al/AlN composite nanoparticles by electrical explosion of aluminum wires in argon and nitrogen. *Powder Technol.*, 2016, **295**, P. 307–314.

[5] Avdeeva Y.A., Luzhkova I.V., Ermakov A.N. Mechanism of formation of nanocrystalline particles with core-shell structure based on titanium oxynitrides with nickel in the process of plasma-chemical synthesis of TiNi in a low-temperature nitrogen plasma. *Nanosystems: Phys. Chem. Math.*, 2022, **13** (2), P. 212–219.

[6] Luzhkova I.V., Ermakov A.N., Grigorov I.G., Zainulin Yu.G., Dobrinskii E.K., Malashin S.I. Plasmachemical processing of titanium carbide and nickelide in a low-temperature nitrogen plasma. *Russ. Metall.*, 2013, **2013**, P. 11–13.

[7] Luzhkova I.V., Ermakov A.N., Murzakaev A.M., Grigorov I.G., Zainulin Yu.G., Dobrinsky E.K., Malashin S.I. Plasma treatment with nickel of vanadium carbide and nitride. *Nanotech. in Russia*, 2014, **9**, P. 667–673.

[8] Kosolapova T.Ya. *Handbook of high temperature compounds: properties, production, applications.* CRC Press, New York, Washington, Philadelphia, London, 1990, 958 p.

[9] Fultz B., Howe J.M. *Transmission electron microscopy and diffractometry of materials*, 3rd ed. Springer, Berlin, Heidelberg, 2008, 758 p.

[10] Ermakov A.N., Luzhkova I.V., Avdeeva Yu.A., Murzakaev A.M., Zainulin Yu.G., Dobrinsky E.K. Formation of complex titanium-nickel nitride Ti0.7Ni0.3N in the "core-shell" structure of TiN – Ni. *Int. J. Refract. Met. Hard Mater.*, 2019, **84**, 104996.

[11] Chalmers B. *Principles of solidification.* John Wiley and Sons, Springer, New York, Dordrecht, Heidelberg, London, 1964, 319 p.

[12] Zhukov M.F., Chersky I.N., Cherepanov A.N., Konovalov N.A., Saburov V.P., Pavlenko N.A., Galevsky G.V., Andrianova O.A., Krushenko G.G. *Strengthening of metallic polymer and elastomer materials with ultradispersed powders obtained by plasma-chemical synthesis*. Nauka, Siberian publishing company of RAS, Novosibirsk, 1999, 307 p. (In Russian)

[13] Shveikin G.P., Alyamovsky S.I., Zainulin Yu.G., Gusev A.I., Gubanov V.A., Kurmaev E.Z. *Variable composition compounds and their solid solutions.* UNTs AN SSSR, Sverdlovsk, 1984, 292 p. (In Russian)
[14] Schuster J.C., Nowotny H. Molybdan- und Molybdan-Wolfram-Carbide im Temperaturbereich von 600 – 1600 °C. *Monatshefte fur Chemie*, 1979, **110**, P. 321–332.
[15] Schönberg N. The Tungsten Carbide and Nickel Arsenide Structures. *Acta Metallica*, 1954, **2**, P. 427–432.
[16] Bhaskar, U.K., Pradhan S.K. Microstructural evolution of nanostructured Ti0.7Ni0.3N prepared by reactive ball-milling. *Mater. Res. Bull.*, 2013, **48**, P. 3129–3135.
[17] Knunyants I.L. *Chemical encyclopedia*: in 5 v. Soviet encyclopedia, Moscow, 1992, **3**, 125 p., 639 p. (In Russian)
[18] Polak L. Elementary chemical processes and kinetics in a non-equilibrium and quasi-equilibrium plasma. *Pure Appl. Chem.*, 1974, **39** (3), P. 307–342.
[19] Borodin V.I.Low-temperature plasma in metal production processes. *Lecture and report materials of the Workshop: Methods and technique of the experimental study of ordered structures self-organization processes in plasma dust formations and the School of young scientists: Topical problems of applications of physics of low-temperature plasma*, 2003, 10 p. (In Russian)
[20] Krzhizhanovsky R.E., Stern Z.Yu. *Thermophysical properties of non-metallic materials (carbides).* Handbook, Energiya, Leningrad, 1976, 120 p. (In Russian)
[21] Barin I. *Thermochemical data of pure substances*. Third edition. VCH, Weinheim, New York, Base1, Cambridge, Tokyo, 1995. 2003 p.

Submitted 20 September 2022; revised 28 November 2022; accepted 5 December 2022

Information about the authors:

Yuliya A. Avdeeva – Institute of Solid State Chemistry, Ural Branch, Russian Academy of Sciences Pervomaiskaya Street, 91, Ekaterinburg, 620990, Russia; ORCID 0000-0002-1470-0476; y-avdeeva@list.ru

Irina V. Luzhkova – Institute of Solid State Chemistry, Ural Branch, Russian Academy of Sciences Pervomaiskaya Street, 91, Ekaterinburg, 620990, Russia; ORCID 0000-0001-9123-5371; key703@yandex.ru

Aidar M. Murzakaev – Institute of Electrophysics, Ural Branch, Russian Academy of Sciences Amundsen Street, 106 Ekaterinburg, 620216, Russia; ORCID 0000-0003-4440-427X; aidar@iep.uran.ru

Alexey N. Ermakov – Institute of Solid State Chemistry, Ural Branch, Russian Academy of Sciences Pervomaiskaya Street, 91, Ekaterinburg, 620990, Russia; ORCID 0000-0002-2746-5292; ermakovihim@yandex.ru

Conflict of interest: the authors declare no conflict of interest.